

Noise-filtering features of transcription regulation in the yeast *S. cerevisiae*

Erik Aurell¹ and Aymeric Fouquier d'Hérouël^{1,2} and Claes Malmnäs¹ and Massimo Vergassola²

¹ Computational Biological Physics, Royal Institute of Technology, AlbaNova University Center, Stockholm, Sweden

² CNRS, URA 2171, Institut Pasteur, Dept. "Génomes et Génétique", Research Unit "Génétique in Silico", 25 rue du Dr Roux, Paris, France

E-mail: eaurell@kth.se, afd@kth.se, malmnas@kth.se, massimo@pasteur.fr

Abstract. Transcription regulation is largely governed by the profile and the dynamics of transcription factors' binding to DNA. Stochastic effects are intrinsic to this dynamics and the binding to functional sites must be controlled with a certain specificity for living organisms to be able to elicit specific cellular responses. Specificity stems here from the interplay between binding affinity and cellular abundance of transcription factor proteins and the binding of such proteins to DNA is thus controlled by their chemical potential.

We combine large-scale protein abundance data in the budding yeast with binding affinities for all transcription factors with known DNA binding site sequences to assess the behavior of their chemical potentials. A sizable fraction of transcription factors is apparently bound non-specifically to DNA and the observed abundances are marginally sufficient to ensure high occupations of the functional sites. We argue that a biological cause of this feature is related to its noise-filtering consequences: abundances below physiological levels do not yield significant binding of functional targets and mis-expressions of regulated genes are thus tamed.

PACS numbers: 87.80.Vt

Running title: *Numbers and affinity*

1. Introduction

A major determinant in transcription regulation is the pattern of transcription factor proteins (TFs) bound in the physical proximity of the transcribed genomic locus [1, 2, 3]. Intense activity is currently carried out to identify transcriptional regulatory networks [4, 5, 6], their topology [7, 8, 9, 10] and signs and strengths of the interactions [11]. Specificity is an obvious need in transcription regulation: functional binding sites ought to be sufficiently low in energy compared to typical sequences in the rest of the genome (the so-called background). This energetic constraint should be coupled with its kinetic counterpart: the TF should be able to rapidly find its functional targets. Existing evidence points at a search taking place via 1D sliding along the DNA, alternated with 3D excursions [12, 13]. The TF is kept along the DNA by non-specific electrostatic interactions, recently characterized experimentally [14, 15].

Two quantitative variables govern the binding of TFs to DNA: their cellular abundance and the affinity between the amino acids forming their binding domains and the various possible stretches of nucleotides. It has long been recognized in concrete examples that equilibrium statistical-mechanics models are poised to describe the binding site occupancy as a function of those parameters, and that these occupancies are proxies for transcription rates transcription [1, 16]. Detailed models for the probability of binding to DNA by TFs have recently been reviewed in [17, 18] and we refer the interested reader thereto (see also Methods for a concise summary).

The qualitative point of importance here is that the probability of TF's binding to DNA is controlled by its so-called chemical potential μ . As illustrated in figure 1, strong binding sites (with energy much lower than μ) are occupied almost certainly, while weak sites, with energies much higher than μ , are most frequently empty. The chemical potential μ increases with the number of copies n of the transcription factor as $\log n$ (see, e.g., [17, 18]). For a single copy $n = 1$, the value of the chemical potential defines an offset F_b , usually called background energy. The reason is that F_b controls the fraction of TF copies bound to DNA either non-specifically or to the genomic background. Indeed, let E^* denote the minimal binding energy, i.e. the energy of binding to the consensus sequence of the TF. From the previous relation $\mu - F_b \propto \log n$, it follows that if $F_b \simeq E^*$, then the threshold defined by the chemical potential μ is larger than (or equals) E^* for any $n \geq 1$. In other words, even a single copy of the transcription factor would then be sufficient to ensure persistent binding, at least of the consensus sequence. Conversely, as F_b becomes less than E^* , more and more TF copies n are needed to have $\mu \geq E^*$, i.e. persistent occupancy of at least the strongest binding sites. A minimal abundance (which depends exponentially on the difference $E^* - F_b$) is then required to have persistent binding of the strongest sites (supposed to be the functional ones).

Detailed quantitative information on the behavior of the chemical potential for transcription factors of biological interest is scanty. The relation between binding affinities and abundances was analyzed in [19] for three coliphage TFs (*Mnt*, *CI* and

Cro) and one bacterial TF (*LacR*). The result was that the offset F_b is comparable to the consensus energy E^* for those four TFs. This type of relation endows the cell with the widest possible window to vary the TF copy number and differentially regulate various sets of genes. It was therefore dubbed “maximum programmability” [19].

Positing $F_b \simeq E^*$ generally valid seems however too strong a requirement for the cellular dynamics, as it would make regulation too prone to errors. In fact, as already noted in [19], the four TFs which were considered are rather special: they are all repressors, they operate without much combinatorial interactions with other factors and their expression is tightly controlled. This is not the situation encountered in general. Namely, combinatorial regulation is much more frequent, especially in eukaryotes, and a large fraction of genes are activated by TFs to their physiological expression levels. Specificity is not arising from a single transcription factor but from the synergistic and cooperative combination of several factors. We then expect that the relation $F_b \simeq E^*$, found in [19] for four particular TFs, does not have general validity and that a different relation holds in the majority of cases. Our goal here is to quantify and support this expectation by analyzing experimental data for a large set of transcription factors.

A good model organism to quantitatively investigate the previous issue is the budding yeast *S. cerevisiae*. Concentration data in the log-growth phase [20] and large-scale chromatin immunoprecipitation binding data, as given by [5, 21], are both available. The intersection of the two data sets leaves us with a set of 63 TFs. The difficulty to be overcome is that large-scale experimental data on binding do not directly provide affinities. *A priori*, calorimetric methods [22, 23] might be employed to measure the strength of the interaction of a TF with its binding sites, but these methods have been hard to scale up, and values are typically not available for a given TF. One is thus forced to infer affinity matrices *in silico*, from a list of experimentally detected binding sites. The procedures and the limitations of these inferences are recalled in the Methods, together with the basics of statistical models for TF-DNA interactions. Two different inference methods were employed: the classical maximum likelihood argument by Berg and von Hippel [24] and the QPMEME method, recently introduced in [25]. Results for the relation between affinity and TF abundance, for both ways of determining the binding energies, are presented hereafter. Biological consequences, in particular for the control of noise in transcription regulation, are presented in the Discussion.

2. Results

Combining the two experimental data sets on abundance [20] and chromatin immunoprecipitation [5, 21], a set of 63 TFs was identified. Affinity matrices for those TFs were then inferred as detailed in Methods, using both the classical maximum likelihood procedure [24] and the QPMEME method [25]. In both cases, the matrices are *a priori* determined only up to a scale factor. In the first case, following [24], the factor was set to one in units of $k_B T$. In the QPMEME method, the scale factor was determined as described in the Methods via a self-consistency condition, based on the

experimental information on TF abundances. This condition could be satisfied in 41 out of the 63 cases. In the remaining 22 cases no solution could be found, for reasons that will be presented in the Discussion.

The matrices derived by the two aforementioned methods agree well in the majority of the 41 cases where both methods could be employed. A first measure of the agreement between two energy matrices is whether they give the best binder at each position, which indeed coincides for 26 TFs out of 41. These 26 instances include cases where one TF admits more than one consensus sequence, but where both matrices agree on at least one consensus binder at each position. In 14 cases the sets of consensus sequences agree completely. For 15 TFs the sets of best binders of the two matrices at some position are not overlapping, *i.e.* in at least one position the sets of best binders differ.

A more quantitative comparison, sensitive to the full energy matrix and not just to the best binder, is to consider the normalized probabilities $q_{i,\alpha}$, *i.e.* the probability that nucleotide α be found at the position i of the DNA-TF binding complex. The probabilities computed using the maximum likelihood procedure [24] or QPMEME [25] are denoted by $q_{i,\alpha}^{\text{BvH}}$ and $q_{i,\alpha}^{\text{QP}}$, respectively. The difference between the two sets of probabilities is quantified by the symmetric Kullback-Leibler relative entropy [26]:

$$S(q_i^{\text{BvH}}, q_i^{\text{QP}}) = \frac{1}{2} \sum_{\alpha} \left(q_{i,\alpha}^{\text{BvH}} - q_{i,\alpha}^{\text{QP}} \right) \log \frac{q_{i,\alpha}^{\text{BvH}}}{q_{i,\alpha}^{\text{QP}}} . \quad (1)$$

Figure 2 shows the mean Kullback-Leibler relative entropy per base pair for the 41 TFs. Except in a few cases, the average differences per base pair are moderate, on the order of 0.1 – 0.2. No correlation was detectable between the relative entropies and the number of observed binding sites employed to infer the affinity matrices, indicating that the differences between the QPMEME and Berg-von Hippel matrices are *bona fide* fluctuations and not due to finite sample effects. Detailed properties of the affinity matrices computed using the two methods are reported in table 1.

As a side remark, note that the average discrimination energy per site generally decreases with the length of the binding site, indicating a trade-off between these two quantities. Figure 3 displays the data for the QPMEME-derived energy matrices; a similar behavior is found for matrices inferred by maximum likelihood.

Figure 4 reports the behavior of the background energy F_b , previously defined as the offset of the chemical potential μ (its value at unit copy number $n = 1$). The result is that the maximum programmability relation $F_b \simeq E^*$ proposed in [19] is indeed peculiar to the three coliphage and the bacterial TFs which were considered. A different behavior is clearly observed in the yeast *S. cerevisiae*. The background energy F_b is not comparable to the consensus binding energy E^* , but is generally smaller and the difference is correlated with the experimentally observed abundancy n_{obs} , as can be seen in figure 4. In other words, the experimental observations are more in agreement with the behavior $E^* - F_b \propto \log n_{\text{obs}}$ than the maximum programmability relation $E^* - F_b \approx 0$. Note that this holds irrespective of the method (maximum likelihood or QPMEME) used to estimate the discrimination matrices.

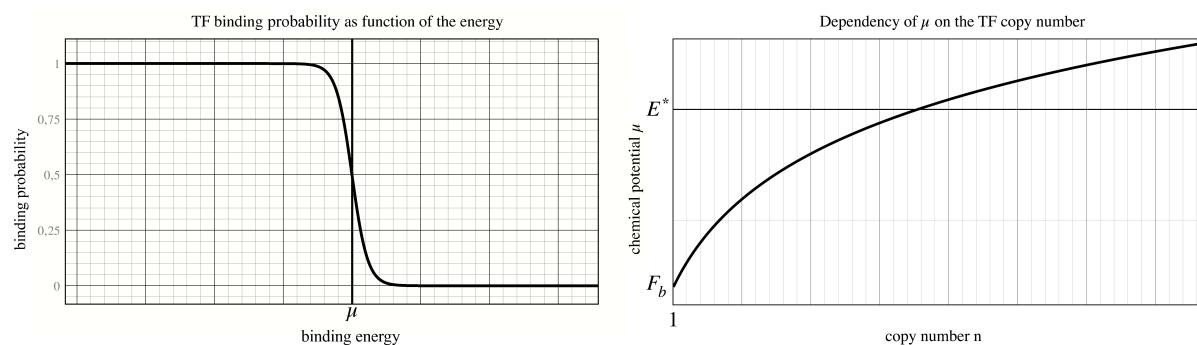


Figure 1. Left panel: A schematic view of the relation between the probability of binding to DNA for a transcription factor and its chemical potential μ . Strong binding sites (with energies much lower than the chemical potential) have a high occupation probability (purple solid line), while the probability to bind decreases rapidly as the energy increases. Right panel: the relation between the chemical potential and the abundance n . The background (free) energy F_b is the value of μ for $n = 1$.

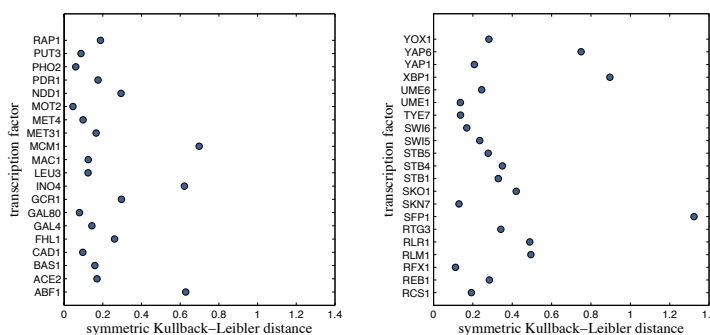


Figure 2. Average Kullback-Leibler distance per base pair between the probability distributions of binding based on computing discrimination energies by maximum likelihood arguments [24] or QPMEME [25] (see also Methods).

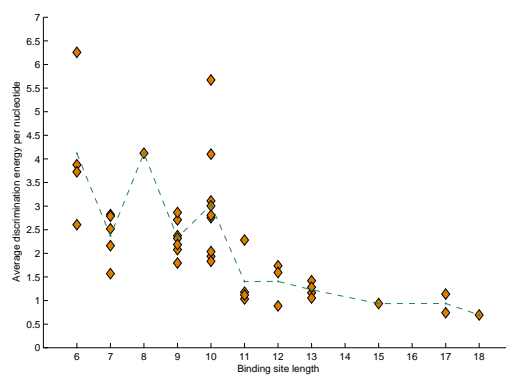


Figure 3. Average discrimination energy *vs* length of binding sites. Reported values refer to energy matrices computed using the QPMEME method, as described in the Methods.

TF name	(a) N_{BS}	(b) n_{obs}	(c) $-r^*$	(d) $ \mu - \langle E_{QP} \rangle $	(e) $E_{QP}^* - \langle E_{QP} \rangle$	(f) $E_{BvH}^* - \langle E_{BvH} \rangle$
ABF1	139	4818.49	1.17	12.86	-15.11	-30.01
ACE2	11	538.41	1.00	17.63	-17.63	-12.65
BAS1	33	861.14	1.00	23.25	-23.25	-15.21
CAD1	8	622.84	1.11	17.51	-19.35	-14.44
DIG1	131	1458.26	1.44	—	—	-16.37
FHL1	75	639.38	1.22	20.60	-25.08	-26.41
FKH1	89	1720.43	1.24	—	—	-19.71
FKH2	53	655.80	1.32	—	—	-23.54
GAL4	9	166.39	1.21	15.89	-19.29	-20.41
GAL80	3	783.80	1.03	12.28	-12.59	-15.10
GCR1	7	258.92	1.13	18.83	-21.36	-12.34
GLN3	48	589.44	1.20	—	—	-18.08
HAP5	22	450.49	1.00	—	—	-11.57
INO2	27	783.80	1.17	—	—	-15.26
INO4	23	521.13	1.20	34.08	-41.01	-18.95
LEU3	9	124.51	1.11	18.42	-20.37	-15.24
MAC1	5	14841.76	1.03	10.71	-10.98	-8.60
MBP1	130	521.13	1.19	—	—	-20.12
MCM1	63	8965.92	1.24	11.06	-13.67	-26.07
MET31	5	521.13	1.00	16.14	-16.14	-10.87
MET4	5	1295.19	1.14	12.34	-14.02	-15.96
MOT2	2	4276.97	1.03	10.31	-10.63	-8.11
MOT3	11	1694.68	1.00	—	—	-9.25
MSN2	14	124.51	1.15	—	—	-14.01
NDD1	27	799.42	1.15	16.10	-18.44	-21.42
NRG1	45	555.55	1.18	—	—	-17.68
PDR1	2	1295.19	1.03	12.51	-12.93	-7.01
PDR3	2	166.39	1.04	—	—	-5.18
PHD1	61	1417.94	1.64	—	—	-15.45
PHO2	3	6418.52	1.09	10.40	-11.37	-8.97
PUT3	3	736.46	1.05	11.85	-12.49	-15.96
RAP1	70	4387.61	1.25	14.60	-18.31	-23.09
RCS1	28	2733.41	1.16	21.04	-24.37	-16.85
REB1	156	7514.31	1.16	13.02	-15.12	-23.68
RFX1	9	376.92	1.11	14.97	-16.66	-18.44
RGT1	12	194.71	1.02	—	—	-12.58
RLM1	9	736.46	1.13	24.46	-27.54	-14.40
RLR1	4	521.13	1.06	19.66	-20.81	-11.10
ROX1	10	238.01	1.03	—	—	-13.49
RTG3	4	1054.72	1.00	15.63	-15.63	-7.43
SFP1	19	258.92	1.21	46.90	-56.71	-17.81
SKN7	64	2572.11	1.25	20.63	-25.77	-18.55
SKO1	8	503.71	1.00	22.35	-22.35	-9.89
SOK2	81	314.38	1.20	—	—	-16.16
SPT23	23	432.40	1.19	—	—	-13.00
SPT2	24	1239.69	1.25	—	—	-16.26
STB1	23	319.30	1.15	27.00	-31.10	-17.94
STB4	4	98.94	1.00	18.69	-18.70	-10.11
STB5	15	279.40	1.12	25.07	-28.06	-16.32
STE12	147	1923.06	1.23	—	—	-18.19
SUM1	43	148.81	1.22	—	—	-20.65
SWI4	99	589.44	1.28	—	—	-21.42
SWI5	40	688.35	1.00	37.53	-37.53	-14.88
SWI6	128	3335.05	1.25	26.45	-32.95	-19.93
TEC1	57	529.79	1.20	—	—	-15.84
TYE7	20	486.13	1.09	19.15	-20.86	-18.00
UME1	2	3037.98	1.04	11.80	-12.27	-7.29
UME6	63	216.63	1.21	24.83	-30.04	-26.54
XBP1	2	194.71	1.00	19.74	-19.74	-5.83
YAP1	11	1616.86	1.06	18.47	-19.66	-13.73
YAP6	3	1350.09	1.00	19.51	-19.51	-6.87
YAP7	48	1694.68	1.09	—	—	-20.14
YOX1	4	861.14	1.10	17.42	-19.11	-10.67

Table 1. Binding parameters for a set of 63 TFs of the yeast *S. cerevisiae*, stating numbers of binding sites used in the analysis (a), experimentally measured protein abundances (b), maximal ratio of binding energy to chemical potential (cf. equation 4 in Methods) (c), and in units of $k_B T$ the estimates for the chemical potential (d) and minimal binding energies (consensus), stemming from both BvH (e) and QPMEME matrices (f), respectively.

As a further test, we compared the experimentally measured TF abundances with the number of binding sites found in SGD [27] and as reported by Lee *et al.* [5]. For the latter, we counted all sites of protein-DNA-interaction with associated p -values $< 1 \cdot 10^{-3}$ (L1) and $< 5 \cdot 10^{-3}$ (L5). The *rationale* of this analysis is as follows. If the maximum programmability ansatz $F_b - E^* \approx 0$ were satisfied, we should expect that TF abundances are the main leverage in the control of the number of binding sites. This is the heuristic advantage provided by maximum programmability [19] and a strong dependence of the number of binding sites on the TF abundance should then be present. No such behavior is expected for the alternative hypothesis $E^* - F_b \propto \log n_{\text{obs}}$: a sizable fraction of the TF copies are weakly attached to the DNA, yet the sites are sufficiently numerous to compete with high-specificity sites. A straightforward regression analysis gives coefficients of regression R^2 close to zero, *viz.* 0.0440 for the SGD set and 0.0513 and 0.0900 for the L1 and L5 sets, respectively. Even though the p -values for the three sets show some statistical significance (0.07, 0.04, 0.006, respectively), the low values of R^2 indicate that the fraction of the variance explained by the regression is scanty. To summarize, the correlation between the number of binding sites and abundance is slightly significant (as should be expected) but the weakness of the dependency confirms previous conclusions.

3. Discussion

The integration of binding data provided by chromatin immunoprecipitation experiments [27, 5] and abundance data from [20] allowed us to extract information on the relation between binding affinities and abundances of TFs in the log-growth phase of the budding yeast *S. cerevisiae*. The availability of experimental data for other conditions would enable a wider perspective, yet two main points have already emerged here and are worth being discussed in their biological consequences and significance.

A first technical point is that, while bioinformatic tools to infer binding free energies generally only give these up to a scale factor, we have shown that combining the recent method QPMEME [25] and abundance data can provide an estimate of that factor. This may be of general methodological interest and useful for future applications.

For the budding yeast problem considered here, the scale factor could be estimated for 41 transcription factors out of 63. For the remaining 22 TFs “individual specificity” is not ensured by the observed affinities and abundances, *i.e.* the binding sites are bound even though their energy is larger than the chemical potential. This prevents using QPMEME, since the method works in the strong binding regime and supposes that all binding sites have energy below the chemical potential. Biologically, having binding sites occupied despite their energies being above the chemical potential does not pose any contradiction, since additional effects such as other factors and/or regulations of the chromosomal structure might crucially contribute to specificity. Indeed, ChIP data (see figure 2 in [5]) clearly indicate that many genes of *S. cerevisiae* are regulated by multiple TFs. Furthermore, global chromatin remodeling effects will reduce the effective size of

the genome which is accessible to TFs and increase specificity. Finally, in eukaryotes it is well known that combinatorial regulation is widespread [3] and its mode of action hinges on strong cooperative effects among the TFs. The corresponding loci are often structured so as to require the synergistic action of various TFs and to remain unbound and inactive if only one of them is present. Results of our analysis are in quantitative agreement with this picture.

The second and main result of our work is that experimentally observed abundances are marginally sufficient to ensure strong and persistent binding of *S. cerevisiae* TFs to DNA sites. This is quantified and supported by the results presented in figure 4. More technically, the background free energy F_b was found to be negative and proportional to $\log n_{\text{obs}}$, where n_{obs} is the abundance experimentally measured in [20]. Consequently, the chemical potential μ remains below the minimal consensus energy E^* if $n \ll n_{\text{obs}}$. This implies that a sizable part of the TF copies are “lost in the background” and that the *in vivo* observed binding sites are only occupied with low probability if the abundance is significantly lower than n_{obs} .

What might superficially appear as a waste, ensures in fact an effective noise-filtering procedure. Fluctuations in the copy number of proteins are unavoidable in the molecular world and have been experimentally demonstrated in various cases (see, e.g., [28]). A few spurious copies of TFs might be present in the cell due to a variety of mechanisms, going from delayed degradations, to leaks or lack of tight regulatory controls and fluctuations in the expression rates. In an *E. coli* system, it has recently been shown that extrinsic effects, over and above cell-cycle dependent changes in gene copy number, acting *e.g.* through different concentrations of metabolites, ribosomes and polymerases, may amount to 35% fluctuations in gene expression levels, and may persist over a cell cycle [29]. Intrinsic fluctuations, while persisting for shorter times, are also significant, at the 20% level [29]. The relation $E^* - F_b \propto \log n_{\text{obs}}$ between the background affinity energy and the abundance of the transcription factors shown in figure 4 ensures an effective way to filter out those fluctuations and control mis-regulations.

4. Conclusions

In conclusion, our results point at the importance of quantitative effects of abundances in the regulatory dynamics of the cell. In particular, the abundance-affinity relationship $E^* - F_b \propto \log n_{\text{obs}}$ demonstrated here is a powerful control lever to ensure global coherent responses of the cellular regulatory networks despite the noisy nature of their individual molecular components.

5. Methods

Let us consider a TF that diffuses in a cell containing a genomic sequence of length L . The partition function of specific and non-specific binding to DNA is

$$Z_b = \sum_{j=1}^L e^{-\beta E(S_j)} + L e^{-\beta E_{\text{ns}}}, \quad (2)$$

where β is the inverse temperature in units of the Boltzmann constant k_B and S_j is the subsequence of length l starting at position j in the genomic sequence. In (2) we have omitted the contribution from the TF freely diffusing in cytoplasm, assuming that number to be much smaller than the number of TFs bound. E_{ns} denotes the energy of the state where the TF is bound non-specifically to the DNA [12, 13, 14]. From (2), it follows the definition of the effective background (free) energy F_b as:

$$F_b = -\beta^{-1} \log Z_b. \quad (3)$$

A commonly employed expression for the binding energies $E(S)$ is the additive *energy matrix* form [30, 31, 32]:

$$E(S) = \sum_{i=1}^l \sum_{\alpha=1}^4 \varepsilon_{i,\alpha} S_{i,\alpha}. \quad (4)$$

Here, the indicator vector $S_{i,\alpha}$ has entries zero or one depending on which nucleotide α stands at position i in the sequence S , $\varepsilon_{i,\alpha}$ is the free energy contribution of nucleotide α at i and l is the length of the binding domain. Even though exceptions are known [33], the linear form (4) generally gives a good approximation of the energy profile [34].

Expression (3) of the background energy F_b may be approximated by an average over a random ensemble (background). The approximation is justified in [19] by a mapping to the Random Energy Model [35]. As for the choice of the random ensemble, the simplest background model features independent nucleotides generated with the average genomic frequencies p_α ($\alpha = A, C, G, T$), yielding:

$$\sum_j e^{-\beta E(S_j)} \simeq L \langle e^{-\beta E} \rangle \equiv L \prod_{i=1}^l \left[\sum_{\alpha} p_{\alpha} e^{-\beta \varepsilon_{i,\alpha}} \right]. \quad (5)$$

It follows that

$$F_b \simeq -\beta^{-1} \log \left\{ L \int dE \rho(E) e^{-\beta E} + L e^{-\beta E_{\text{ns}}} \right\}, \quad (6)$$

where $\rho(E) = \langle \delta \left(E - \sum_{i,\alpha} \varepsilon_{i,\alpha} S_{i,\alpha} \right) \rangle$ is the density of states for the random ensemble. The background density $\rho(E)$ can be computed by a saddle point expansion, where the first term is Gaussian [25]. Figure 5 compares the empirical energy density (obtained by the histogram of the energies measured over the whole genome) with the Gaussian and the first correction. While the former alone would not be appropriate (the empirical curve is not symmetric), the correspondence with the latter is quite fair. For a few TFs the match is less good, mainly because discretization effects are more pronounced.

For a TF present with n copies in the cell, the probability that a sequence S_i be bound by the TF takes the Fermi-Dirac form (see, e.g., [19, 17, 18] for more details):

$$\mathcal{P}(S_i) = \frac{1}{1 + e^{\beta(E(S_i) - \mu)}}, \quad (7)$$

with the chemical potential μ implicitly defined by

$$n = L \int dE [\rho(E) + \delta(E - E_{\text{ns}})] \frac{1}{1 + e^{\beta(E - \mu)}}. \quad (8)$$

Equation (8) simply states that the sum over all the binding sites, weighted by the probability that a TF is bound there, equals the copy number of the TF in the system.

5.1. Inference of binding properties

A list of binding sites for a wide set of TFs of *S. cerevisiae* was downloaded from the SGD database [27]. The binding sites were extracted from the intergenic regions identified by chromatin immunoprecipitation experimental data [5] as detailed in [21]. We retained those TFs for which at least two binding sites and their abundance were available and processed them as detailed hereafter.

A proxy of the binding properties of the TFs is provided by the log-odds ratios based on the classical work [24]:

$$\Delta\varepsilon_{i,\alpha} = \frac{1}{\lambda} \log \frac{1 + n_i^*}{1 + n_{i,\alpha}}, \quad (9)$$

where $n_{i,\alpha}$ is the number of observations of nucleotide α at the i -th position in the binding site and n_i^* is the number of observations of the most frequently observed nucleotide in that position. λ is an unknown scale factor in units of $k_B T$.

The discrimination energy of a sequence S is defined as the difference between $E(S)$ and the consensus energy and is hence directly given by $\Delta\varepsilon_{i,\alpha}$ in (9). The scale factor λ must be determined from at least one experimentally measured affinity. In the absence of experimental data, we have set it to unity (in units of $k_B T$), which is a fair average of the values found for a number of prokaryotic examples in [24], and concurs with bioinformatic practice [34].

As a second proxy we have used the recently introduced QPMEME method [25]. This also does not give access to the binding energies as such, but to the ratio of binding energies to a chemical potential, shifted by the mean free energy of binding of the corresponding TF:

$$r \equiv \frac{E - \langle E \rangle}{|\mu - \langle E \rangle|} \equiv \frac{\hat{E}}{|\hat{\mu}|} = \sum_{i,\alpha} \hat{\varepsilon}_{i,\alpha} S_{i,\alpha}, \quad (10)$$

where $\langle \bullet \rangle$ denotes the average over the random background ensemble defined as before. The calculation of the matrix $\hat{\varepsilon}_{i,\alpha}$ boils down to a convex optimization problem, where the width of the background probability distribution is minimized under the constraints that all sequences in the training set be bound. Note that neither the average energy $\langle E \rangle \equiv \sum_{i,\alpha} p_{i,\alpha} \varepsilon_{i,\alpha}$ nor the chemical potential μ are determined by QPMEME.

Differences between pairs of energies, *e.g.* discrimination energies, are determined up to the scale factor $|\hat{\mu}|$.

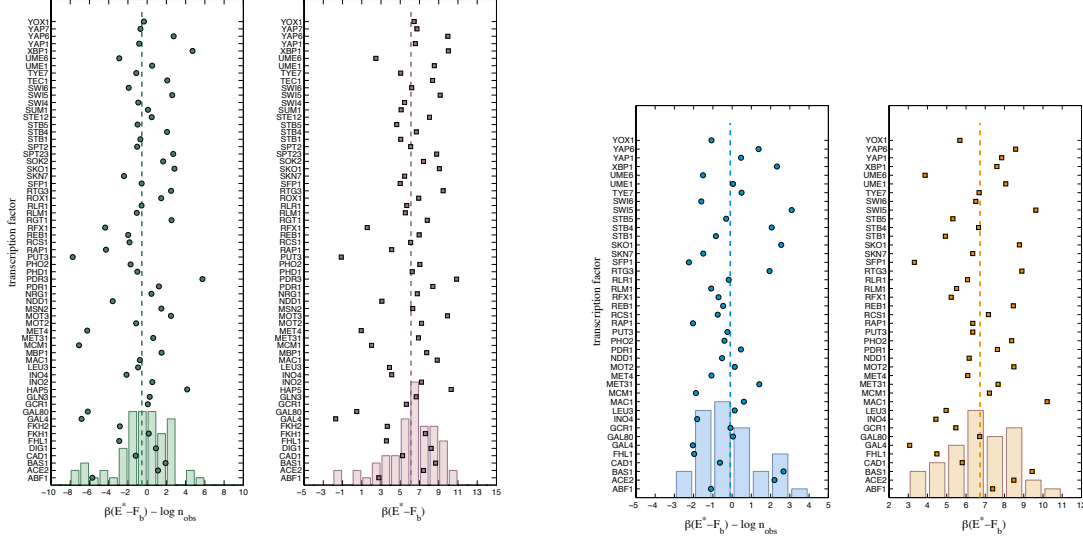


Figure 4. Comparison of the relation between the background energy F_b and the abundance for a set of *S. cerevisiae* transcription factors. Values of the difference between the consensus energy E^* and the background energy F_b are reported as squares. Their values shifted by the logarithm of the TF abundance (as measured experimentally) are reported as circles. Vertical dashed lines correspond to the average values for the two sets of points. Points have a sizeable scatter but circles are clearly centered around zero. No relation has been found between the deviation of the points around zero and the functional role of the corresponding TFs. Long panels: results for log-odds ratio matrices; short panels: results for QPMEME matrices. Histograms give better visual access to the distribution widths.

The energy matrices $\Delta\varepsilon_{i,\alpha}$ and $\hat{\varepsilon}_{i,\alpha}$ have finite sample errors, which could in principle be estimated as in [24]. Assuming the sample to be non-biased, these errors decrease with the number of known binding sites N_{BS} as $1/\sqrt{N_{BS}}$. A comparison with table 1 reveals that this error is at least on the order of 10% (for those TFs for which about a hundred binding sites are known), ranging up to 50% (for those with only a few binding sites known). The chemical potential is determined by the reduced energy matrix and the observed abundance n_{obs} , which also has experimental errors and is likely to fluctuate *in vivo*. An estimate of the error in the estimation of the chemical potential is thus at best on the order of 10%. This should nevertheless be sufficient to elucidate statistical trends, which is our purpose here.

The probabilities $q_{i,\alpha}$ appearing in the Results denote the probabilities that nucleotide α is found at position i in the TF-DNA complex. They are computed from the energy matrices $\Delta\varepsilon_{i,\alpha}$ as:

$$q_{i,\alpha} = \frac{e^{-\beta\Delta\varepsilon_{i,\alpha}}}{\sum_{\alpha'} e^{-\beta\Delta\varepsilon_{i,\alpha'}}}. \quad (11)$$

5.2. Computing the background free energy

Definition (3) involves two terms: one describing binding to the genomic background and the other non-specific electrostatic interactions with the DNA. The latter is crucial to the target search [12]. As shown in [19], the background contribution cannot be larger than the non-specific part: the TF would otherwise diffuse in the background random medium and get slowed down by its local minima. In fact, the two contributions are expected to be comparable. The division in background and functional binding sites is indeed dynamical and the former provides the evolutive reservoir for the latter. Therefore, evolvability of the regulatory network suggests that the background energy will tend to be low, compatibly with the aforementioned specificity and kinetic constraints (see [36, 37] about evolvability).

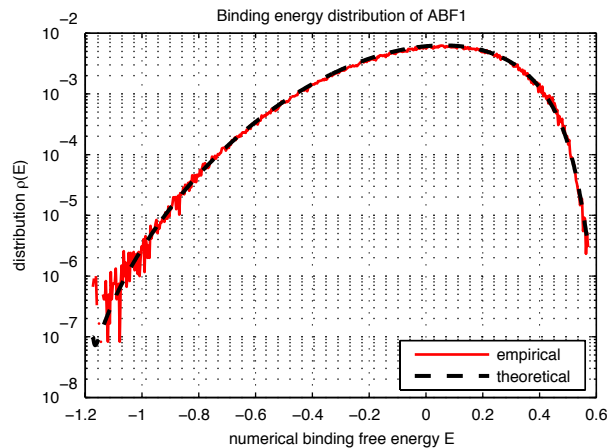


Figure 5. The density of states for the TF ABF1. Dashed in black, the curve obtained for a random background. In red, the empirical curve found by computing the distribution of energies over the genome. The energy scale has been chosen so as to have the chemical potential $\mu = -1$.

Our estimate for the background energy F_b in (6) is then:

$$\beta(E^* - F_b) = \log \left[2L \int dr \rho(r) e^{-(\beta|\hat{\mu}|)(r-r^*)} \right]. \quad (12)$$

Here, $\rho(r)$ is the background density of states for the energy matrix $\hat{\epsilon}_{i,\alpha}$ obtained by QPMEME and r^* is the minimal value of the ratio (10), that is for the energy E^* of the consensus sequence(s) S^* . The shift to E^* in (12) is introduced just to facilitate comparison with the results in figure 4.

The quantity $\beta|\hat{\mu}|$ is not determined by the QPMEME method proper. We estimate it using the relation (8), the fact that in QPMEME binding energies are only determined up to the relative chemical potential, and the additional information on the TF abundance n_{obs} from [20]. Using the previous arguments on background and non-specific contributions, we get:

$$n_{\text{obs}} = 2L \int dr \rho(r) \frac{1}{1 + e^{\beta|\hat{\mu}|(r+1)}}, \quad (13)$$

whence $\beta|\hat{\mu}|$ is extracted and inserted back into (12) to obtain the value of the background effective (free) energy F_b . As previously discussed, (13) only has a solution for 41 cases out of 63 TFs. It is instructive to compare with (8), which has a solution for every TF. The chemical potential μ then simply acts as a cut-off, so that sites with energies lower than μ are mostly bound, while sites with higher energies are not, and the total number of bound TFs equals n_{obs} . Depending on n_{obs} , the mostly unbound sites could or could not include *in vivo* observed binding sites *i.e.*, part of the set of sites from which the maximum likelihood energy matrices have been constructed. In (13), on the other hand, all the *in vivo* binding sites must necessarily have binding energy below the chemical potential, because these are the constraints under which the QPMEME reduced energy matrix $\hat{\varepsilon}$ is determined. Hence, all sites for which the reduced QPMEME reduced energy is below the threshold -1 will be at least half-filled. Each of these is actually present in the genome with some probability, which leads to a total expected number of at least half-filled sites. Therefore, (13) cannot be solved if n_{obs} is low enough, because the right-hand side has a lower bound. This happens in about one third of the cases at hand.

5.3. Maximal programmability

In the simplest scenario where the major contribution in (8) stems from energies where the Fermi-Dirac weight can be approximated by the Boltzmann factor, one can invert (8) to obtain

$$\mu \simeq \beta^{-1} \log n + F_b. \quad (14)$$

The occupation probability of a site t reads then $P_t = \frac{1}{1+\tilde{n}_t/n}$, where the threshold concentration \tilde{n}_t is $e^{\beta(E_t - F_b)}$. The minimal copy number required for strong binding (to the consensus) must then be at least $e^{\beta(E^* - F_b)}$.

Maximal programmability [19] amounts to positing the lowest (unity) threshold. The approximate equality $F_b \approx E^*$ should then hold. One consequence, which motivates the term, is that the consensus sequence is then half-bound if there is just a single copy of the TF present in the cell. Different regulatory elements can then have threshold set, or programmed, from one, if their sequences are the consensus sequence, and upwards, independently of a feedback induced by the actual TF copy number.

Acknowledgements

This work was supported by the Swedish Research Council through contract 2003-4614 (E.A., C.M and A.F.d'H.).

References

- [1] M. Ptashne. *A genetic switch (3rd edition)*. Cold Spring Harbour Laboratory Press, 2005.

- [2] E.H. Davidson, J.P. Rast, P. Oliveri, A. Ransick, C. Calestani, C.-H. Yuh, T. Minokawa, G. Amore, V. Hinman, C. Arenas-Mena, O. Otim, C.T. Brown, C.B. Livi, P.Y. Lee, R. Revilla, A.G. Rust, Z.J. Pan, M.J. Schilstra, P.J.C. Clarke, M.I. Arnone, L. Rowen, R.A. Cameron, D.R. McClay, L. Hood, and H. Bolouri. A genomic regulatory network for development. *Science*, 295:1669–1678, March 2002.
- [3] E.H. Davidson. *Genomic Regulatory Systems*. Academic Press, 2001.
- [4] B.F. Pugh and D.S. Gilmour. Genome-wide analysis of protein-dna interactions in living cells. *Genome Biology*, 2:1013.1–1013.3, 2001.
- [5] T.I. Lee, N.J. Rinaldi, F. Robert, D.T. Odom, Z. Bar-Joseph, G.K. Gerber, N.M. Hannett, C.T. Harbison, C.M. Thompson, I. Simon, J. Zeitlinger, E.G. Jennings, H.L. Murray, D.B. Gordon, B. Ren, J.J. Wyrick, J.B. Tagne, T.L. Volkert, E. Fraenkel, D.K. Gifford, and R.A. Young. Transcriptional regulatory networks in *saccharomyces cerevisiae*. *Science*, 298:799–804, 2002.
- [6] L.A. Boyer, T.I. Lee, M.F. Cole, S.E. Johnstone, S.S. Levine, J.P. Zucker, M.G. Guenther, R.M. Kumar, H.L. Murray, R.G. Jenner, D.K. Gifford, D.A. Melton, R. Jaenisch, and R.A. Young. Core transcriptional regulatory circuitry in human embryonic stem cells. *Cell*, 122:1–10, 2005.
- [7] R. Milo, S. Shen-Orr, S. Itzkowitz, N. Kashtan, D. Chklovskii, and U. Alon. Network motifs: simple building blocks of complex networks. *Science*, 298:824–827, 2002.
- [8] S. Shen-Orr, R. Milo, S. Mangan, and U. Alon. Network motifs in the transcriptional regulation network of *escherichia coli*. *Nat Genet.*, 31:64–8, May 2002.
- [9] H.-W. Ma, B. Kumar, U. Ditges, F. Gunzer, J. Buer, and A.-P. Zeng. An extended transcriptional regulatory network of *escherichia coli* and analysis of its hierarchical structure and network motifs. *Nucleic Acids Research*, 32:6643–6649, 2004.
- [10] A. Mazurie, S. Bottani, and M. Vergassola. An evolutionary and functional assessment of regulatory network motifs. *Genome Biology*, 6:R35, 2005.
- [11] M. Ronen, R. Rosenberg, B.I. Shraiman, and U. Alon. Assigning numbers to the arrows: Parameterizing a gene regulation network by using accurate expression kinetics. *P.N.A.S.*, 99:10555–10560, 2002.
- [12] P.H. von Hippel and O.G. Berg. Facilitated target location in biological systems. *J. Biol. Chem.*, 264:675, 1989.
- [13] S.E. Halford and J.F. Marko. How do site-specific dna-binding proteins find their targets? *Nucleic Acids Res.*, 32:3040–3052, 2004.
- [14] M. Slutsky and L.A. Mirny. Kinetics of protein-dna interaction: Facilitated target location in sequence-dependent potential. *Biophys. J.*, 87:4021, 2004.
- [15] D.M. Gowers, G.G. Wilson, and S.E. Halford. Measurement of the contributions of 1d and 3d pathways to the translocation of a protein along dna. *PNAS*, 102:15883–15888, 2005.
- [16] M.A. Shea and G.K. Ackers. The or control system of bacteriophage lambda. a physical-chemical model for gene regulation. *J Mol Biol.*, 182:211–30, January 1985.
- [17] L. Bintu, N.E. Buchler, H.G. Garcia, U. Gerland, T. Hwa, J. Kondev, T. Kuhlman, and R. Phillips. Transcriptional regulation by the numbers: models. *Curr Opin Genet Dev.*, 15:116–24, 2005.
- [18] L. Bintu, N.E. Buchler, H.G. Garcia, U. Gerland, T. Hwa, J. Kondev, T. Kuhlman, and R. Phillips. Transcriptional regulation by the numbers: applications. *Curr Opin Genet Dev.*, 15:125–35, 2005.
- [19] U. Gerland, J.D. Moroz, and T. Hwa. Physical constraints and functional characteristics of transcription factor-dna interaction. *Proc Natl Acad Sci U S A*, 99:12015–20, 2002.
- [20] S. Ghaemmaghami, W. Huh, K. Bower, R.W. Howson, A. Belle, N. Dephoure, E.K. O’Shea, and J.S. Weissman. Global analysis of protein expression in yeast. *Nature*, 425:737–741, 2003.
- [21] C.T. Harbison, D.B. Gordon, T.I. Lee, N.J. Rinaldi, K.D. Macisaac, T.W. Danford, N.M. Hannett, J.B. Tagne, D.B. Reynolds, J. Yoo, E.G. Jennings, J. Zeitlinger, D.K. Pokholok, M. Kellis, P.A. Rolfe, K.T. Takusagawa, E.S. Lander, D.K. Gifford, E. Fraenkel, and R.A. Young. Transcriptional regulatory code of a eukaryotic genome. *Nature*, 431:99–104, 2004.
- [22] Z. Zhang and T. Palzkill. Determinants of binding affinity and specificity for the interaction

- of tem-1 and sme-1 beta-lactamase with beta-lactamase inhibitory protein. *J. Biol. Chem.*, 278:45706–45712, 2003.
- [23] Y. Takeda, A. Sarai, and V.M. Rivera. Analysis of the sequence-specific interactions between cro repressor and operator dna by systematic base substitution experiments. *Proc. Natl. Acad. Sci. USA*, 86:439–443, 1989.
- [24] O.G. Berg and P.H. von Hippel. Selection of dna binding sites by regulatory proteins: Statistical-mechanical theory and application to operators and promoters. *J. Mol Biol.*, 193:723–750, 1987.
- [25] M. Djordjevic, A. M. Sengupta, and B.I. Shraiman. A biophysical approach to transcription factor binding site discovery. *Genome Res*, 13:2381–2390, 2003.
- [26] T.M. Cover and J.A. Thomas. *Elements of Information Theory*. Wiley-Interscience, 2006.
- [27] R. Balakrishnan, K.R. Christie, M.C. Costanzo, K. Dolinski, S.S. Dwight, S.R. Engel, D.G. Fisk, J.E. Hirschman, E.L. Hong, R. Nash, R. Oughtred, M. Skrzypek, C.L. Theesfeld, G. Binkley, C. Lane, M. Schroeder, A. Sethuraman, S. Dong, S. Weng, S. Miyasato, R. Andrada, D. Botstein, and J. M. Cherry. Saccharomyces genome database. <http://www.yeastgenome.org/>, last visited September 12, 2005.
- [28] M.B. Elowitz, A.J. Levine, E.D. Siggia, and P.S. Swain. Stochastic gene expression in a single cell. *Science*, 297:1183–1186, 2002.
- [29] Nitzan Rosenfeld, Jonathan W. Young, Uri Alon, Peter S. Swain, and Michael B. Elowitz. Gene regulation at the single-cell level. *Science*, 307:1962 – 1965, 2005.
- [30] G.D. Stormo, T.D. Schneider, L. Gold, and A Ehrenfeucht. Use of the perceptron algorithm to distinguish translational initiation sites in e. coli. *Nucleic Acids Res.*, 10:2997–3011, 1982.
- [31] R. Staden. Computer methods to locate signals in nucleic acid sequences. *Nucleic Acids Res.*, 12:505–19, 1984.
- [32] G.D. Stormo. Dna binding sites: representation and discovery. *Bioinformatics*, 16:16–23, 2000.
- [33] M.L. Bulyk, P.L. Johnson, and G.M. Church. Nucleotides of transcription factor binding sites exert interdependent effects on the binding affinities of transcription factor. *Nucleic Acids Res.*, 30:1255–61, 2002.
- [34] G.D. Stormo and D.S. Fields. Specificity, free energy and information content in protein-dna interactions. *TIBS*, 23:109–113, 1998.
- [35] B. Derrida. Random-energy model – an exactly solvable model of disordered systems. *Phys. Rev. B*, 24:2613–2626, 1981.
- [36] J. Berg, S. Willmann, and M. Lassig. Adaptive evolution of transcription factor binding sites. *BMC Evol. Biol.*, 4:Art. No. 42, 2004.
- [37] V. Mustonen and M. Lassig. Evolutionary population genetics of promoters: Predicting binding sites and functional phylogenies. *P.N.A.S.*, 102:15936–15941, 2005.